Molecular Biology of the Cell
Vol. 18, 3545–3555, September 2007

The Insulin-like Growth Factor-I–mTOR Signaling Pathway Induces the Mitochondrial Pyrimidine Nucleotide Carrier to Promote Cell Growth[D]

Suzanne Floyd,* Cedric Favre,* Francesco M. Lasorsa,† Madeline Leahy,* Giuseppe Trigiante,* Philipp Stroebel,‡ Alexander Marx,‡ Gary Loughran,* Katie O'Callaghan,* Carlo M.T. Marobbio,† Dirk J. Slotboom,§ Edmund R.S. Kunji,§ Ferdinando Palmieri,† and Rosemary O'Connor*

*Cell Biology Laboratory, Department of Biochemistry, BioSciences Institute, National University of Ireland, Cork, Ireland; †Department of Pharmaco-Biology, Laboratory of Biochemistry and Molecular Biology, University of Bari, and Consiglio Nazionale delle Ricerche Institute of Biomembranes and Bioenergetics, 70125 Bari, Italy; ‡Institute of Pathology, University Hospital Mannheim, University of Heidelberg, D68135 Mannheim, Germany; and §Medical Research Council, Dunn Human Nutrition Unit, Cambridge CB2 2XY, United Kingdom

Submitted December 15, 2006; Revised June 11, 2007; Accepted June 14, 2007
Monitoring Editor: Carl-Henrik Heldin

The insulin/insulin-like growth factor (IGF) signaling pathway to mTOR is essential for the survival and growth of normal cells and also contributes to the genesis and progression of cancer. This signaling pathway is linked with regulation of mitochondrial function, but how is incompletely understood. Here we show that IGF-I and insulin induce rapid transcription of the mitochondrial pyrimidine nucleotide carrier PNC1, which shares significant identity with the essential yeast mitochondrial carrier Rim2p. PNC1 expression is dependent on PI-3 kinase and mTOR activity and is higher in transformed fibroblasts, cancer cell lines, and primary prostate cancers than in normal tissues. Overexpression of PNC1 enhances cell size, whereas suppression of PNC1 expression causes reduced cell size and retarded cell cycle progression and proliferation. Cells with reduced PNC1 expression have reduced mitochondrial UTP levels, but while mitochondrial membrane potential and cellular ATP are not altered, cellular ROS levels are increased. Overall the data indicate that PNC1 is a target of the IGF-I/mTOR pathway that is essential for mitochondrial activity in regulating cell growth and proliferation.

INTRODUCTION

Insulin and insulin-like growth factor-I (IGF-I) regulate metabolism and cell survival, growth, and proliferation through the insulin or IGF-I receptors (IR or IGF-IR) and their downstream signaling pathways. Increased IGF-IR expression and activity have been associated with many human cancers (LeRoith and Roberts, 2003), and overexpression of the IGF-IR in murine tumor models promotes an invasive and metastatic phenotype (Lopez and Hanahan, 2002). Some of the most frequently altered tumor-suppressor genes or oncogenes in cancers encode proteins that directly affect the highly conserved signaling pathway from the IGF-IR via the Insulin Receptor Substrate (IRS) adapter proteins to the lipid kinase phosphoinositide 3-kinase (PI3-K), the serine threonine kinase Akt, and the serine threonine kinase mTOR (mTORC1 and mTORC2 complexes). PI-3 kinase and Akt can both act as oncogenes, whereas tumor suppressors that regulate this pathway include the lipid phosphatase PTEN, the tuberous sclerosis complex (TSC1/TSC2), the LKB1 kinase, and the DNA damage–activated tumor suppressor p53 (Schmelzle and Hall, 2000; Altomare and Testa, 2005; Cully *et al.*, 2006; Samuels and Ericson, 2006). Unsurprisingly, there is significant interest in targeting the IGF-IR and components of its signaling pathway for the treatment of cancer (Hofmann and Garcia-Echeverria, 2005).

The role of IGF-I signaling and Akt in regulating energy metabolism and glycolysis in tumor cells is receiving renewed attention. Tumor cells have long been recognized to have the ability to metabolize glucose and produce ATP rapidly through enhanced rates of glycolysis. This phenotype associated with increased production of lactic acid was described by Warburg in the 1920s (Warburg, 1924, 1930), and it can be detected using positron emission tomography (PET). Enhanced glycolysis is thought to confer cancer cells with a distinct competitive edge over normal cells by providing adequate ATP for rapid proliferation under hypoxic conditions and has also been proposed to protect cells from oxidative stress (Brand and Hermfisse, 1997). One of the ways in which the PI3-K and Akt pathway promotes cell survival and tumor growth is to stimulate glucose metabolism. Activated Akt increases levels of cell surface transporters for glucose (Plas *et al.*, 2001; Edinger and Thompson, 2002; Plas and Thompson, 2005) and also regulates the expression and location of mitochondrial hexokinases, which

This article was published online ahead of print in *MBC in Press* (http://www.molbiolcell.org/cgi/doi/10.1091/mbc.E06–12–1109) on June 27, 2007.

[D] The online version of this article contains supplemental material at *MBC Online* (http://www.molbiolcell.org).

Address correspondence to: Rosemary O'Connor (r.oconnor@ucc.ie).

catalyze the first step of glycolysis (Majewski *et al.*, 2004). A direct role for mTOR signaling in enhancing mitochondrial oxidative phosphorylation has also recently been described (Schieke *et al.*, 2006) as well as a role for mTOR in regulating the production of mitochondrial-derived reactive oxygen species (ROS) that are thought to be causative in ageing (Schieke and Finkel, 2006).

Although much evidence points to altered mitochondrial physiology in cancer cells, the interactions between growth factor signaling and mitochondrial function in regulating cell survival and proliferation remain to be fully elucidated. For this reason we sought to investigate the function of a previously uncharacterized mitochondrial carrier protein that was identified in a screen for genes whose expression is increased in cells transformed by overexpressing the IGF-IR (R+ cells). These cells were generated from a fibroblast cell line derived from the IGF-IR knockout mouse (R− cells) by re-expressing the IGF-IR (Sell *et al.*, 1994). The differential screen of genes expressed in R+ and R− cells identified a group of genes generally associated with cancer cell metabolism and migration (Loughran *et al.*, 2005a,b) and a group of genes of unknown function, which included the mitochondrial carrier protein.

Mitochondrial carrier proteins link metabolic pathways in mitochondria and the cytosol by transporting nucleotides, metabolites, and cofactors through the otherwise impermeable inner mitochondrial membrane. They are required for the generation of energy; amino acid synthesis and degradation; intramitochondrial DNA, RNA, and protein synthesis; and other fundamental cellular functions (Kaplan, 2001; Kunji, 2004; Palmieri, 2004).

The mitochondrial carrier is located on chromosome 1 and shares significant identity with the essential yeast mitochondrial carrier Rim2p (YBR192W; Van Dyck *et al.*, 1995; Marobbio *et al.*, 2006). Its expression is dependant on activation of the PI-3 kinase and mTOR pathways and is enhanced in transformed cell lines and primary tumors compared with normal cells and tissues. Like Rim2p (Marobbio *et al.*, 2006), the carrier transports pyrimidine nucleotides and was designated PNC1 (pyrimidine nucleotide carrier 1). Overexpression of PNC1 in MCF-7 cells caused an increase in cell size and suppression of PNC1 expression caused a decrease in cell size in several cell lines, as well as decreased cell cycle progression and proliferation of MCF-7 cells. Mitochondrial UTP levels were significantly reduced when PNC1 expression was suppressed. These observations suggest that the IGF-I-PI3-K-mTOR signaling pathway controls mitochondrial function directly and that PNC1 is important for mitochondrial activity in regulating cell growth (cell size) and proliferation.

MATERIALS AND METHODS

Cloning of PNC1

The expressed sequence tag clone of mouse *pnc1* was obtained from the IMAGE consortium. To generate full-length *pnc1* for cloning in frame with green fluorescent protein (GFP) at the C terminus oligonucleotide primers for *pnc1* were designed incorporating the restriction sites XhoI and ApaI. The sequence of these oligonucleotides is as follows: m*pnc1* forward primer 5′ GCGCTCGAGGCGGGCCATGGCG 3′; m*pnc1* reverse primer 5′ GGCGGGC-CCAGTAAGCACGCTC 3′. The PCR products were ligated into the pEGFPC1 plasmid that had been digested with XhoI and ApaI. The pcDNA3 vector encoding Ha-mPNC1 was generated by ligating the insert from pEGFPC1-PNC1 into a modified version of the pcDNA3 plasmid encoding the Ha peptide. To generate the bacterial expression vector pRUN, the coding sequence for human *pnc1* (h*pnc1*) was amplified by PCR from testis cDNA, and the NdeI and HindIII restriction sites were introduced for ligation into pRUN. The sequences of all PCR products were verified by DNA sequencing.

The promoter sequence of the *pnc1* gene encompassing a region of 3 kbp upstream of the transcription start site (+1) was extracted from the Ensembl database (Gene ID: ENSG00000171612). Putative transcription factor binding sites were identified in this sequence by analysis using the TFSEARCH version 1.3 program (http://www.cbrc.jp/research/db/TFSEARCH.html), which compared the sequence with a database of identified transcription factor binding sites (TRANSFAC databank (Heinemeyer *et al.*, 1998).

Cell Culture, IGF-I/Insulin Stimulation, and Transfection

MCF-7 breast carcinoma cells, R− cells, R+ cells, and DU145 and HeLa cells were all maintained in DMEM supplemented with 10% (vol/vol) fetal bovine serum (FBS), 10 mM L-glutamine, and antibiotic (all from Biowhittaker, Verviers, Belgium), which was designated complete medium (CM). HeLa cells were transiently transfected with pcDNA3 encoding Ha-PNC1 or empty pcDNA3 vector (4 μg of DNA) using LipofectAMINE 2000 (Invitrogen, Paisley, United Kingdom). To generate stable transfectants, MCF-7 cells were cultured in medium containing G418 (Calbiochem, Nottingham, United Kingdom; 1 mg/ml), and individual clones were selected and screened for expression of Ha-PNC1 by Western blotting. To analyze signaling response cells were starved from FBS before stimulation with IGF-I (100 ng/ml, PeproTech, Rocky Hill, NJ). To analyze *pnc1* mRNA expression, cells were grown to a confluence of ~70%, serum-starved (for 4 h for R+ cells and for 12 h for MCF-7 and R− cells), and then stimulated with either IGF-I or insulin. To inhibit signaling pathways cells were incubated with 30 μm PD98059 (MAP kinase inhibitor), 20 μm LY294002 (PI-3 kinase inhibitor), or 100 nM rapamycin (mTOR inhibitor) for 30 min before stimulation with IGF-I. All inhibitors were from Calbiochem.

Northern Blot Analysis

Total RNA was isolated from R− and R+ cells using Trizol Reagent (Invitrogen) according to the manufacturer's instructions, separated on 1.5% (wt/vol) denaturing formaldehyde gels, and transferred to nylon membranes (Hybond-N, Amersham, Buckinghamshire, United Kingdom). A murine multiple tissue Northern blot was obtained from Clontech. α-^{32}P-labeled *pnc1* probes (1×10^6 cpm/ml) were generated by the random oligonucleotide primer method (NEBlot: New England Biolabs, Hertfordshire, United Kingdom). Prehybridization and hybridization were carried out at 42°C in 50% formamide, 5× SSC, 4× Denhardt's solution, 0.1% SDS, and salmon sperm DNA (100 μl/ml, Sigma, Dublin, Ireland) for 2 and 1 5 h, respectively. Filters were washed twice at 42°C using 2× SSC, 0.1% SDS for 5 min, and then twice at 42°C using 0.5× SSC and 0.1% SDS for 15 min, before being scanned for signal using a phosphorimager.

Immunofluorescence and Flow Cytometry Assays

For immunofluorescence, cells on cover slips were washed with phosphate-buffered saline (PBS) and placed in serum-free DMEM with 25 nM mitoTracker dye (Molecular Probes, Hamburg, Germany) for 30 min. Cells were fixed in 3.7% formaldehyde in PHEM buffer (60 mM Pipes, 25 mM HEPES, 10 mM EGTA, 2 mM $MgCl_2$, pH 6.9) for 10 min and permeabilized with 0.1% Triton X-100 in PHEM for 5 min. For staining with the anti-Ha antibodies, cells were first preblocked with 2.5% normal goat serum in PHEM for 30 min and then incubated with primary antibody, washed with PHEM, and incubated with Cy2-conjugated secondary antibody (Jackson ImmunoResearch Laboratories, Newmarket, United Kingdom). Cells were examined using a Nikon fluorescent microscope (Kingston upon Thames, United Kingdom).

Mitochondria mass was assessed by first fixing cells in PBS containing 2% formaldehyde and 2% glutaraldehyde for 30 min at 37°C, followed by incubation in PBS containing 25 nM MitoTracker dye (Molecular Probes) for 30 min. Cells were washed and analyzed by flow cytometry. Cellular ROS were assessed by incubating cells in PBS containing 10 μM H_2DCF-DA fluorescent probe (Molecular Probes) for 15 min in the dark at 20°C.

For cell cycle analysis, cells were trypsinized, resuspended in cold PBS containing 200 μg/ml RNAse A (Sigma), and kept on ice. Before analysis by flow cytometry, NP-40 and propidium iodide (Sigma) were added at a final concentration of 0.1% and 50 μg/ml, respectively. DNA content was measured in the FL2 channel of a flow cytometer using the CellQuest software (Becton Dickinson, Oxford, United Kingdom).

Assays for Cell Proliferation and Cell Size

Cells were cultured in CM at 3×10^4 cells per well in a 24-well plate. To monitor cell growth, cells were removed at the indicated times to Eppendorf tubes using trypsin-EDTA and centrifuged at $1000 \times g$ for 3 min. The cell pellets were then resuspended in 100 μl of medium and counted using trypan blue exclusion.

To determine relative cell size, cells in six-well plates were transfected with *pnc1*-specific siRNA. After incubation for 24 h cells were trypsinized and reseeded into 60-mm plates at ~30% confluence in CM. Rapamycin (Calbiochem; 100 nM) was added to some cultures 24 h after reseeding. At the indicated times, cells were removed from the plates using trypsin and resuspended for fluorescence-activated cell sorting (FACS) analysis. In each sample 10,000 cells were analyzed by flow cytometry using CellQuest software to obtain the mean forward scatter height (FSC-H).

Cellular Protein Extracts and Western Blotting

Cellular protein extracts were prepared by lysing in lysis buffer (Tris-HCl, pH 7.4, 150 mM NaCl, 1% Nonidet P-40) plus the tyrosine phosphatase inhibitor Na_3VO_4 (1 mM) and the protease inhibitors phenylmethylsulfonyl fluoride (1 mM), pepstatin (1 μm), and aprotinin (1.5 μg/ml). After incubation at 4°C for 20 min, nuclear and cellular debris were removed by microcentrifugation at 20,000 × *g* for 15 min at 4°C. For Western blot analysis proteins were resolved by SDS-PAGE on 4–15% gradient gels and transferred to nitrocellulose membranes. Blots were incubated for 1 h at room temperature in tris-buffered saline (TBS) containing 0.05% Tween 20 (TBS-T) and either 5% milk (wt/vol) or 2% bovine serum albumin (BSA). This was followed by primary antibody incubations overnight at 4°C. The anti-phospho p70 S6 Kinase Thr 389 and anti-phospho p70 S6 Kinase Thr 421/Ser 424, anti-p70 S6 Kinase, anti-phospho-4E-BP1, anti-phospho-Akt, anti-Akt and anti-phospho-p42/44 MAP kinase antibodies were all from Cell Signaling Technology (Beverly, MA). Anti-mitogen-activated protein kinase 2 (MAPK2) and anti-paxillin were from Upstate Biotechnology (Lake Placid, NY). The anti-Ha antibody 12CA5 was from Roche Molecular Biochemicals (East Sussex, United Kingdom) and anti-VDAC antibody was from Santa Cruz Biotechnology (Santa Cruz, CA). The anti-actin mAb was from Sigma. Secondary antibodies conjugated with horseradish peroxidase (Dako, High Wycombe, United Kingdom) were used for detection with enhanced chemiluminescence (ECL, Amersham Biosciences, Little Chalfont, United Kingdom).

Small Interfering RNA Oligonucleotides and Transfection

Small interfering RNAs (siRNAs; Elbashir *et al.*, 2001) oligonucleotides were obtained from MWG (Ebersberg, Germany). An oligonucleotide complementary to both the human and mouse sequence of the *pnc1* gene (aatttggttggagttgcacca; corresponding to nucleotides 311–332 in the human gene and nucleotides 304–325 in the mouse gene after the start codon) was used. Two other predesigned oligonucleotides specific for the human gene were obtained from Ambion (Huntingdon, United Kingdom; siRNA1 ID no. 123672 and siRNA3 ID no. 123673). A negative control siRNA (negative control no. 1) was also from Ambion. Transfection was carried out using OligofectAMINE transfection reagent (Invitrogen) with concentrations of oligonucleotide ranging from 10 to 200 nM. All concentrations tested showed similar specific effects on suppressing protein expression and decreasing cell size. For most experiments 50 nM of oligonucleotide was used. Expression of the transfected Ha-PNC1 protein was assessed by Western blotting using the anti-Ha antibody. RNA levels were assessed using semiquantitative or quantitative RT-PCR 48–96 h after transfection.

Semiquantitative and Quantitative RT-PCR

Tissue extracts from prostate carcinomas and macrodissected adjacent normal prostate were isolated from radical prostatectomy specimens directly after surgery. All samples were used after informed consent of the patient and approval by the local Ethics Committee of the University of Würzburg, Germany. Total RNA was isolated using the Trizol method and cDNA synthesis was carried out by reverse transcription with equal amounts of RNA (2 μg) using a cDNA synthesis kit (Roche Molecular Biochemicals or Invitrogen). Equal amounts of cDNA were amplified and the quantity of reverse transcription reaction used for amplification was nonsaturating for the PCR product after the selected number of amplification cycles.

Quantitative PCR was carried out using the ABI Prism 7900HT Sequence Detection System (Applied Biosystems, Foster City, CA; or in the case of prostate tissues by the LightCycler instrument; Roche Molecular Biochemicals) with QuantiTect SYBR Green technology (Qiagen, Crawley, West Sussex, United Kingdom). Primers used were as follows: *pnc1*: 5′-GCTCTGCAGCTTTTATCACAAATTC-3′ and, 5′-AACGTAACGAGCACACTGGAGTG-3′; *gapdh*: 5′-CCCATGTTCGTCATGGGTGTGA-3′ and 5′-TGGTCATGAGTCCTTCCACGATACC-3′; *β-actin*: 5′-ATTGCCGACAGGATGCAGAA-3′ and 5′-GCTGATCCACATCTGCTGGAA-3′. Plates were heated for 15 min at 95°C, and 40 PCR cycles consisting of 15 s at 95°C, 30 s at 60°C, and 30 s at 72°C were applied. Samples were subsequently heated to 95°C. Results were expressed as DeltaDelta C_T $[(C_T \text{ PNC1} - C_T\text{GAPDH})_{siRNA} - (C_T\text{PNC1} - C_T\text{GAPDH})_{neg}]$ and as relative amounts to negative control.

Purification of PNC1 from Escherichia coli

hPNC1 was expressed in inclusion bodies in *E. coli* BL21(DE3) cells using procedures previously described for the bovine oxoglutarate carrier (Fiermonte *et al.*, 1993) and several other mitochondrial carriers (Palmieri *et al.*, 2000). Control cultures containing the empty pRUN vector were processed in parallel. Inclusion bodies were purified on a sucrose density gradient (Fiermonte *et al.*, 1993) and washed at 4°C first with buffer A (10 mM Tris-HCl, pH 7.0/0.1 mM EDTA); twice with 3% (wt/vol) Triton X-114, 1 mM EDTA, and 10 mM Pipes/NaOH, pH 7.0; and finally with buffer A. The proteins were solubilized in 1.8% (wt/vol) *N*-dodecanoylsarcosine (sarkosyl). Small residues were removed by centrifugation.

Reconstitution into Liposomes and Transport Measurements

The recombinant hPNC1 protein in sarkosyl was reconstituted into liposomes in both the presence and the absence of substrates, as described previously (Palmieri *et al.*, 1995). The external substrate was removed from proteoliposomes on Sephadex G-75 columns pre-equilibrated with 50 mM NaCl and 10 mM PIPES, pH 7.0. Transport at 25°C was started by adding the indicated labeled substrate and was stopped after 90 min by adding a mixture of 20 mM pyridoxal 5′-phosphate and 20 mM bathophenanthroline. In control samples the inhibitors were added at time zero according to the inhibitor stop method (Palmieri *et al.*, 1995), the external radioactivity was removed, and the radioactivity in the liposomes was measured. The experimental values were corrected by subtracting the respective controls.

Mitochondrial Isolation

Cells were removed from plates by trypsinization followed by washing with PBS and centrifugation at 1000 × *g* to generate a pellet. A volume of mitochondrial extraction buffer (10 mM Tris-Cl, pH 7.5, 210 mM sucrose, 70 mM sorbitol, 10 mM NaCl, 1 mM EDTA, 1.5 mM $MgCl_2$) equivalent to three times the volume of the pellet was added. Cells were homogenized by fine needle (26-gauge) aspiration 10 times and the homogenates centrifuged at 1000 × *g* for 15 min at 4°C. The supernatants were removed to fresh tubes and recentrifuged at 1000 × *g* to remove any residual cellular contaminants. The supernatants were again removed and centrifuged at 7000 × *g* for 15 min at 4°C. The pellet obtained represents the mitochondrial fraction. This was then washed three times with PBS to remove any remaining cytosolic fraction contaminants.

Extraction and Analysis of Nucleotides

The cell or mitochondrial pellet was gently resuspended in an ice-cold 6% solution of trichloroacetic acid to precipitate protein. Samples were incubated on ice for 10 min and centrifuged at 20,800 × *g* for 10 min at 4°C. The protein pellet was discarded, and, to remove the acid, an equal volume of 7.0% trioctylamine in Freon (1,1,2 trichlorotrifluoroethane) was added to the retained supernatant. The mixture was shaken vigorously and then centrifuged at 20,800 × *g* for 5 min at 4°C. The nucleotides were recovered in the upper aqueous phase.

Chromatographic separation of the nucleotide pools was achieved using reverse phase, ion-pairing HPLC on a Vydac C18 column (250 × 4.6 mm, 5-μm particle size) fitted with a C18 guard column. The mobile phase consisted of buffer A (4.0 mM tetrabutylammonium bisulphate, 100 mM KH_2PO_4, pH 6.0) and buffer B, which was prepared by adding 30% methanol to buffer A. Buffers were filtered and degassed before use. Separation was achieved at 1 ml/min using the following gradient: 0–20% buffer B over 8 min, 20–70% B over 12 min, and then a decrease to 0% B over 5 min. Nucleotide standard solutions, prepared using a 5′-nucleotide and nucleoside kit from Sigma, were used to validate peak positions.

RESULTS

Expression of a Mitochondrial Carrier Is Enhanced in IGF-IR–transformed Fibroblasts

Suppressive subtractive hybridization (SSH) was used to isolate cDNAs that were differentially expressed between the R− and R+ cell lines (Loughran *et al.*, 2005b). The mRNA for one of the cDNAs was confirmed by Northern blotting to be more abundantly expressed in R+ cells than in R− cells (Figure 1A). This cDNA was used to probe a multiple tissue blot, which showed high expression of mRNA in liver and testis, lower levels in heart and brain, but undetectable levels in spleen, lung, skeletal muscle, or kidney (Figure 1B).

A comparison of both the human and mouse sequences with those in the EMBL Nucleotide Sequence database showed that this cDNA encoded a member of the mitochondrial carrier family (Palmieri, 1994; Kunji, 2004). These carriers have three homologous repeats, each containing a signature motif, typically P-X-[DE]-X-X-[KR] (Figure 1C). The main structural fold is a six α-helical bundle with pseudo-threefold symmetry as exemplified by the structure of the bovine ADP/ATP carrier (Pebay-Peyroula *et al.*, 2003). This gene is located on human chromosome 1 (1p36.22), and its product (Q9BSK2) has another isoform (Q96CQ1) with 60% identity that is located on chromosome 3. It is also identical in sequence to a previously reported human carrier of unknown function huBMSC-MCP that was assigned to chromosome 11 (Wang *et al.*, 2004). Both isoforms have homologues in mice, Q921P8 and Q922G0 with 91 and 61% shared identity with PNC1, respectively. These carriers contain a

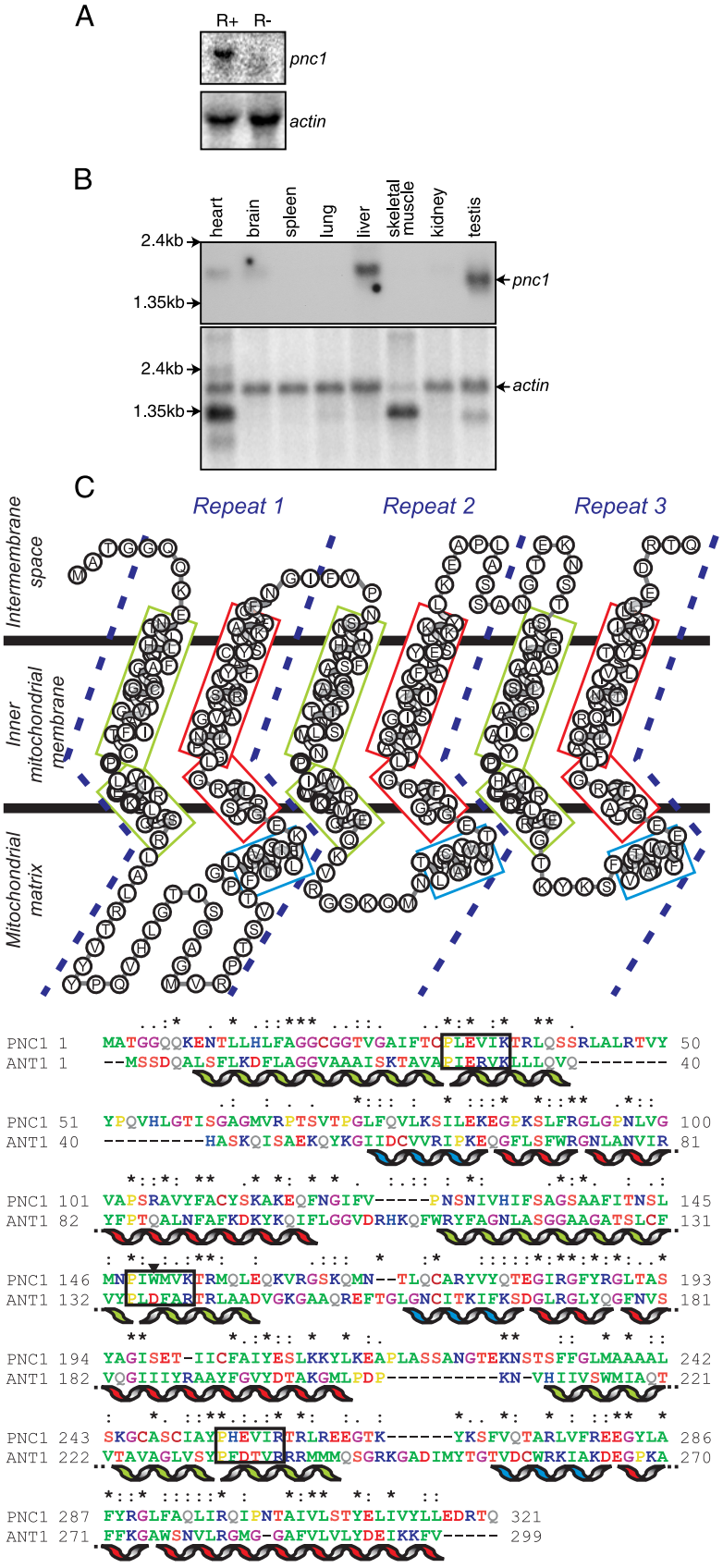

Figure 1. Pnc1 mRNA is abundant in R+ cells compared with R− cells and encodes a mitochondrial carrier protein. (A) RNA was isolated from R+ and R− cells and used to generate Northern blots. This blot and a murine multiple tissue blot (B) were probed with radiolabeled probes derived from the murine *pnc1* cDNA. Both were reprobed for actin expression to demonstrate RNA loading. (C) The predicted protein topology of the mitochondrial pyrimidine transporter PNC1 based on the homology to the bovine ADP/ATP carrier (Pebay-Peyroula *et al.*, 2003), showing the six transmembrane α-helices, the threefold sequence repeats and the conserved signature motifs. Also shown is the alignment of PNC1 with the bovine ADP/ATP carrier ANT1, showing identical residues (*) and similar ones (. and :), the positions of the α-helices, and the signature motifs (box).

deviation in the signature motif of the second repeat, where the negatively charged amino acid has been replaced by a tryptophan (P-I-W-M-V-K), but the basic residue of the interacting salt bridge is retained. The π-electrons of the aromatic residues form a negatively charged face, which can interact electrostatically with positively charged residues (Dougherty, 1996) The human mitochondrial carrier is also closely related to three carriers from yeast—Rim2p or Pyt1p (Marobbio *et al.*, 2006), Ndt1p, and Ndt2p (Todisco *et al.*, 2006)—that share an identity of 29.5, 23.4, and 24.0%, respectively.

pnc1 *Expression Is Enhanced in Transformed Cells and Is Induced by IGF-I or Insulin*

pnc1 mRNA is overexpressed in R+ cells compared with R− cells, so this suggested that its expression level and related transport activity are important determinants of its contribution to metabolism in R+ cells and other transformed cells.

To investigate this, we asked if *pnc1* expression was associated with cellular transformation in cells other than fibroblasts. *pnc1* mRNA was detected in the breast carcinoma cell line MCF-7, but not in the nontumorigenic breast myoepithelial cell line MCF10A (Figure 2A). Similarly *pnc1* mRNA was detected in the Jurkat T lymphocytic leukemia cell line, but not in primary T lymphocytes (Figure 2A). *pnc1* mRNA expression was then investigated in a panel of 11 primary prostate carcinomas compared with normal prostate tissue. Significantly higher *pnc1* expression was observed in the prostate tumors compared with normal tissues (Figure 2B).

Next we investigated whether *pnc1* expression was regulated by IGF-I or insulin. R+ cells were starved of serum, then stimulated with IGF-I, and analyzed by Northern blotting for *pnc1* expression. In R+ cells *pnc1* mRNA was low in starved cells but was rapidly induced after 4 h of IGF-I stimulation (Figure 2C). In MCF-7 cells *pnc1* mRNA expression was induced by 4-h stimulation with IGF-I (Figure 2C), with a further increase after 24 h. R− cells were used to investigate whether *pnc1* transcription was responsive to insulin. *pnc1* mRNA expression was not detectable in starved R− cells but was induced by insulin after 2 and 4 h, and a further induction was observed after 8 and 12 h (Figure 2C). A similar pattern of *pnc1* induction was observed in the 3T3L1 preadipocyte cell line (data not shown).

Induction of *pnc1* mRNA by IGF-I in MCF-7 cells was found to be dependent on the activity of the PI-3 kinase and mTOR pathways, but it was repressed by the Erk MAPK pathway. This was determined by pharmacological inhibition of each of these three pathways with LY29004 (PI3 kinase inhibitor), rapamycin (mTOR inhibitor), and PD98059 (Mek inhibitor) before IGF-I stimulation (Figure 2D). Examination of the PNC1 promoter region revealed that in addition to the classical promoter components such as the TATA box, CBP/p300, and S8 ribosome unit binding sites a large number of putative binding sites for transcription factors responsive to the PI-3K, mTOR, MAPK, and PKA pathways were evident (Supplementary Figure S1).

Taken together these data indicate that *pnc1* expression is enhanced in transformed cell lines and primary tumors and is rapidly responsive to either insulin or IGF-I signaling through the PI-3 kinase/mTOR pathway.

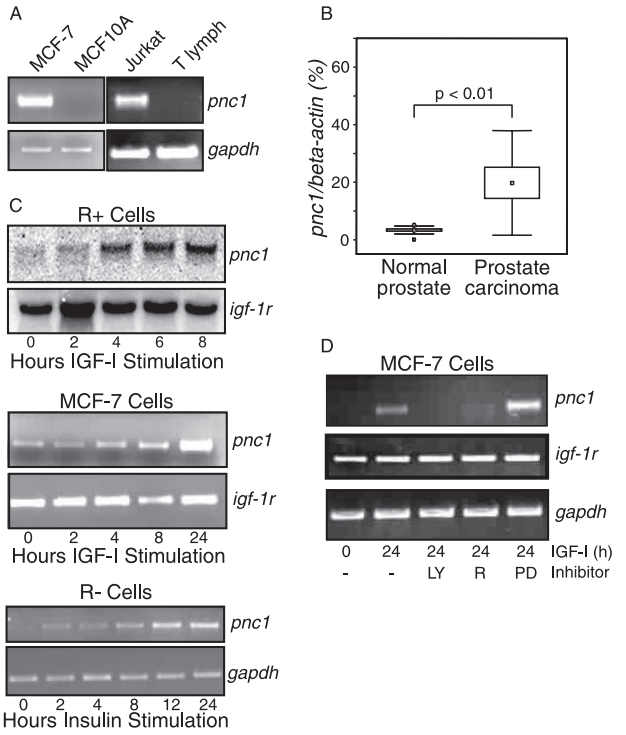

Figure 2. Pnc1 mRNA expression in cells and induction by IGF-I and insulin. (A) MCF-7 and MCF-10A cells were cultured in complete medium, and RT-PCR was carried out on isolated RNA using *pnc1*-specific primers or *gapdh* primers. (B) RNA was extracted from a panel of 11 prostate carcinomas and 11 normal prostate tissues derived from the same patients and analyzed by quantitative PCR (qPCR) using *pnc1*-specific primers and *β-actin* primers as a control. The data are presented as the mean and SD of PNC1 compared with β-actin for the 11 samples. Statistical significance was determined ($p < 0.01$) using the Mann-Whitney U and Wilcoxon 2 sample test. (C) R+ cells were starved from serum and stimulated with IGF-I (100 nM) for the indicated times at which RNA was isolated. Northern blots were probed with radiolabeled human *pnc1* cDNA and for *actin*. MCF-7 cells were serum-starved and then stimulated with IGF-I for the indicated times at which times RNA was isolated for semiquantitative RT-PCR using *pnc1*-specific primers. As a control RT-PCR from the same samples was carried out using primers directed to the kinase domain of the *igf-1r*. R− cells were serum-starved and stimulated with 10 nM insulin for the indicated times, and RNA was isolated for RT-PCR using *pnc1* and *gapdh* primers. (D) MCF-7 cells were pretreated with either PD98059 (MAP kinase inhibitor), LY294002 (PI-3 Kinase inhibitor), or rapamycin (mTOR inhibitor) for 30 min before IGF-I stimulation. At the indicated times RNA was isolated for RT-PCR.

Overexpressed PNC1 Causes an Increase in Cell Size

To investigate if overexpression of the PNC1 protein could be used to determine its contribution to IGF-I and insulin signaling in tumor cells, plasmids encoding PNC1 as either a GFP- or Ha-fusion protein were transiently transfected into MCF-7 or HeLa cells. Confocal microscopy showed that GFP-PNC1 colocalized with mitoTracker, which specifically labels mitochondria (Figure 3A). HeLa cells transiently expressing Ha-PNC1 were costained with an anti-Ha antibody and a human anti-mito antibody, which labels mitochondrial membranes. This demonstrated that Ha-PNC1 became localized to mitochondrial membranes. Overexpression of PNC1 had no discernible effect on mitochondrial membrane polarization as assessed with the JC1 fluorescent probe (data not shown), which indicates that it does not alter the integrity of the mitochondrial membrane.

The effects of PNC1 levels on cell size were assessed in clones of MCF-7 cells that stably overexpressed PNC1. MCF-7/Ha-PNC1 cells consistently exhibited an increased light scatter compared with Neo cells, which is indicative of in-

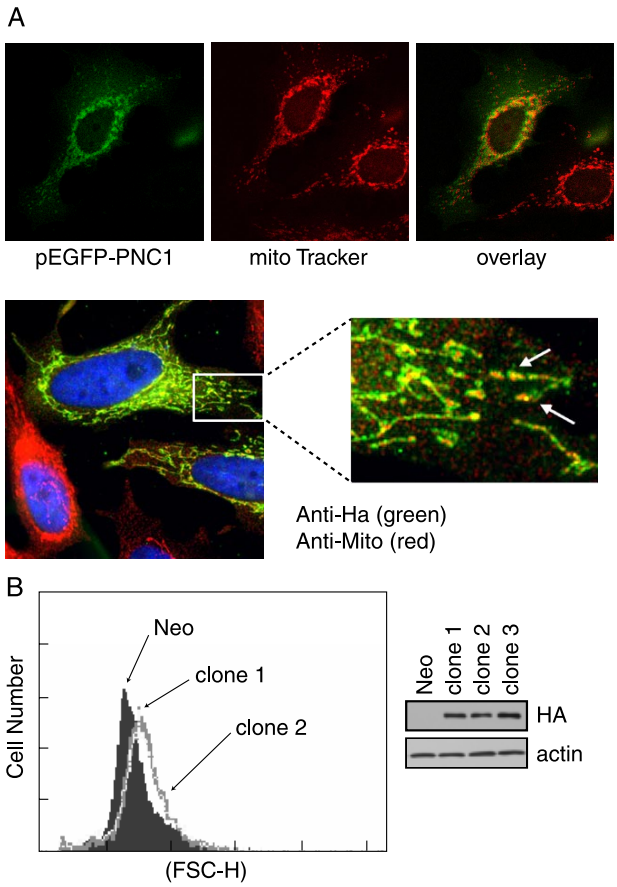

Figure 3. PNC1 is localized to the mitochondrial membrane and causes an increase in cell size. (A) MCF7 cells were transiently transfected with pEGFPN1-PNC1 and then incubated with 25 nM mitotracker dye. Cells were fixed, and images were obtained with a confocal microscope. HeLa cells were transiently transfected with Ha-PNC1 and then were immunolabeled with the anti-Ha antibody (green) and the human anti-mito antibody (red). (B) MCF-7 cells were transfected with the pcDNA vector encoding Ha-PNC1 or empty vector, and clones of each transfected pool were isolated. FACS analysis was used to assess cell size of MCF-7/Ha-PNC1 cells compared with vector controls. The solid graph represents the control cells, whereas the empty graph represents MCF-7/HaPNC1 cells. These are representative of several analyses of cells at different stages of culture in complete medium. The expression levels of the Ha-PNC1 protein are shown in the inset. Western blots of lysates were prepared from MCF-7 cells.

creased cell size (increased cell growth; Figure 3B). MCF-7/Ha-PNC1 cells cultured in either 10% FBS, IGF-I, or insulin showed very little difference in proliferation compared with the control cells expressing only the vector (not shown).

Suppression of PNC1 by siRNA Causes Decreased Cell Size and Decreased Proliferation

Because mitochondrial carrier proteins have low turnover rates and are present in the mitochondrial membrane at low levels (Palmieri, 1994), we hypothesized that suppression of PNC1 expression could have a greater impact on cells than overexpression of the protein. This hypothesis is supported by the observation that Rim2p yeast mutants exhibit a petite phenotype in complete medium (Van Dyck *et al.*, 1995).

Several siRNA oligonucleotides directed against *pnc1* were used to suppress its expression in MCF-7, MCF-7/Ha-PNC1, DU145 prostate carcinoma, or HeLa cervical carcinoma cell lines. We could not generate rabbit antisera with sufficiently high affinity to detect endogenous PNC1 protein, so the Ha antibody was used to detect overexpressed PNC1 protein and RT-PCR was used to detect endogenous *pnc1* mRNA. Ha-PNC1 protein expression was reduced at 2, 3, and 4 d in MCF-7/HaPNC1 cells transfected with *pnc1*-specific siRNA compared with control (Figure 4A). RT-PCR analysis demonstrated that endogenous *pnc1* mRNA was reduced in siRNA-treated MCF-7/Neo cells, but mRNAs for the folate and dicarboxylate mitochondrial carriers (Fiermonte *et al.*, 1998; Titus and Moran, 2000) were not altered (shown in Figure 4B at 72 h after transfection).

Cell size was reduced in MCF-7/Neo, MCF-7/Ha-PNC1 cultures at 48, 72, and 96 h after transfection with *pnc1*-specific siRNA compared with mock-transfected cells (Figure 4C). As a control, cells were treated with rapamycin, which causes decreased cell size through inhibition of mTOR. Rapamycin had a similar effect on cell size as the *pnc1*-specific siRNA in MCF-7/Neo cells and had a smaller effect than *pnc1* siRNA on cell size in MCF-7/HaPNC1 cells. Cell size was also reduced by siRNA-mediated reduction of PNC1 expression in DU145 cells and HeLa cells (Figure 4C).

Proliferation of MCF-7 cell cultures transfected with *pnc1*-specific siRNA was greatly decreased over 96 h compared with control siRNA-transfected cells (Figure 4D). Analysis of cell cycle progression in MCF-7 cells demonstrated that cells with PNC1 suppressed had more cells in the G1 phase of the cell cycle and fewer cells in the G2/M phases than control cells (Figure 4E). This indicates that the cell cycle is delayed in the G1 phase in cell cultures with reduced PNC1 expression, which may explain the reduced growth (size) and proliferation of these cells. Overall, these data demonstrate that reduced PNC1 expression causes retarded cell growth and proliferation.

IGF-I–mediated Activation of mTOR Is Not Affected by PNC1 Expression

Our data demonstrate that suppression of PNC1 reduces cell growth and proliferation. The effect on cell growth in MCF-7 cells was similar to the effects of the mTORC1 inhibitor rapamycin. Because both growth factors and nutrients are necessary for activation of the mTORC1 pathway, we hypothesized that PNC1 may contribute to a mitochondria-dependent signal required for mTOR activation. Therefore, we investigated the status of the mTOR pathway in cells with enhanced or suppressed PNC1 expression. As can be seen in Figure 5 IGF-I-mediated phosphorylation of Akt and the mTORC1 target proteins S6K1 and 4EBP1 was not altered in MCF-7 cells overexpressing PNC1. Moreover, suppression of PNC1 expression in MCF-7 or HeLa had no effect on IGF-I–mediated phosphorylation of these proteins (data not shown). Altogether these results indicate that the effect of PNC1 on cell size and proliferation is not due to altered IGF-I–mediated activation of the mTORC1 pathway.

PNC1 Transports Pyrimidine Nucleotides with Preference for UTP

Our data indicate that PNC1 is essential for cell growth, so we next sought to determine what substrate PNC1 transports into the mitochondria that might mediate its function in promoting cell growth. To investigate the substrate specificity of PNC1 transport assays were carried out after reconstitution of the purified recombinant protein into liposomes. The transport activity was tested in homo-exchange experiments, which have the same substrate on both sides of the membrane. The recombinant transporter catalyzed active

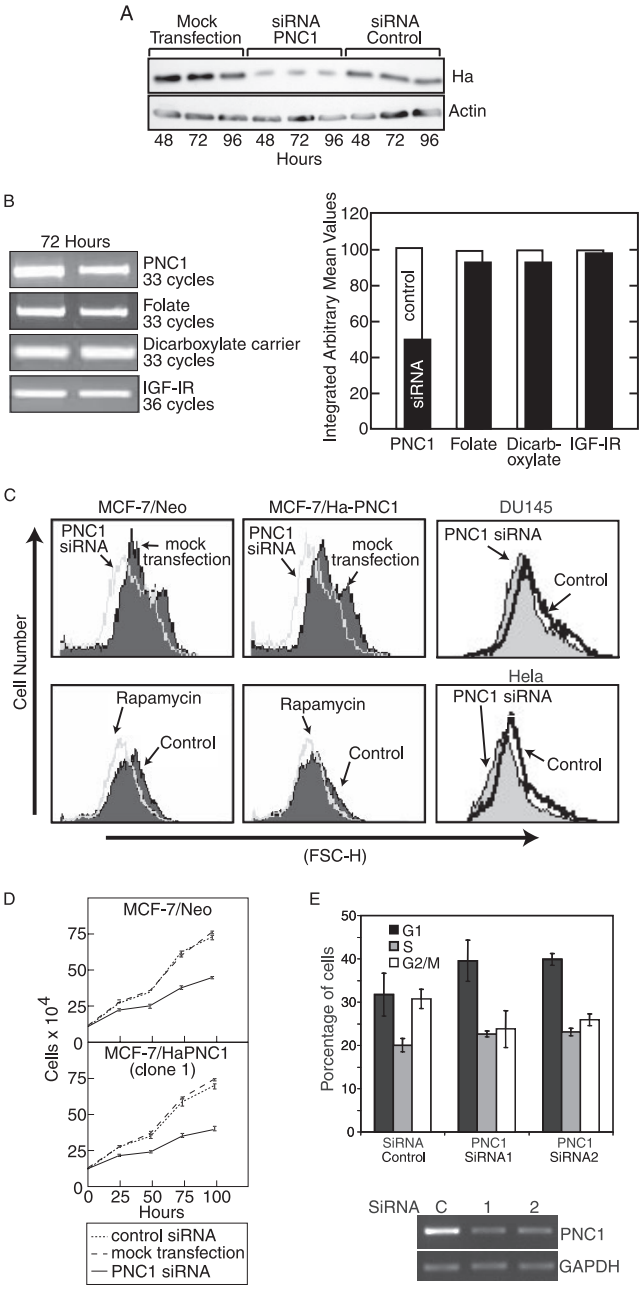

Figure 4. Knockdown of *pnc1* with siRNA reduces cell size and proliferation in MCF-7 cells. MCF-7/Ha-PNC1 and MCF-7/Neo cells were transfected with siRNA oligonucleotides directed toward human and mouse *pnc1*, with a control siRNA or with oligofectamine alone (mock). (A) Western blot analysis of cell lysates prepared from MCF-7/Ha-PNC1 cells transfected with siRNA oligonucleotide directed toward human and mouse *pnc1*, control siRNA, or mock transfection at 48, 72, and 96 h. (B) Semiquantitative RT-PCR showing level of *pnc1* mRNA in MCF-7/Neo cells at 72 h after transfection with *pnc1* siRNA. Levels of mRNA for the folate and dicarboxylate mitochondrial carriers and the IGF-IR are also shown to measure specificity of siRNA. The bar charts represent the relative mean volume of the mRNA levels shown in the gels. (C) MCF-7/Neo, MCF-7/Ha-PNC1, DU145, and HeLa cells were transfected with siRNA directed to *pnc1* or mock transfected. MCF-7/Neo and MCF-7/Ha-PNC1 cells were also treated with rapamycin or were left untreated. Cell size was measured by analysis of forward light scatter (FSC-H) by flow cytometry 72 h after transfection. (D) Cell proliferation rates were assessed in MCF-7/Neo and MCF-7/PNC-1 cells at 24, 48, 72, and 96 h after siRNA transfection. (E) MCF-7 cells were transfected with a control siRNA (SiRNA C) or two siRNAs targeting PNC1 (SiRNA 1, 2). After 72 h cells were stained with propidium iodide and analyzed by flow cytometry for DNA content. Data are presented as the average percentage of cells in G1, S, or G2/M phases of the cell cycle from three separate experiments. Expression levels of *pnc1* and *gapdh* mRNA were determined by RT-PCR for each transfected cell population and are shown in the bottom panels.

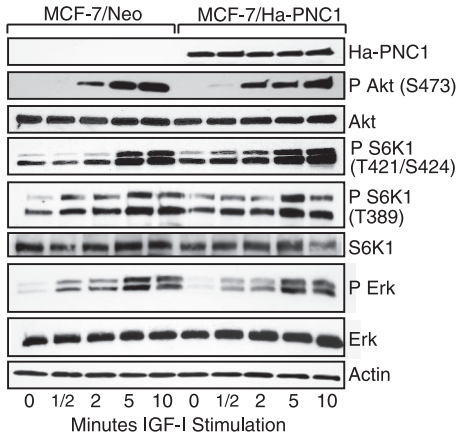

Figure 5. Effects of PNC1 overexpression on mTOR pathway. MCF-7/Neo and MCF-7/Ha-PNC1 cells were starved for 4 h and then stimulated with IGF-I for the indicated times. Lysates were prepared and analyzed by Western blotting with anti-phospho-Akt (S473), anti-phospho-Erk, and anti-phospho S6K1 Kinase antibodies (Thr 389 and Thr 421/Ser424). The blots were also reprobed with anti-Akt, anti-HA, anti-S6K1, anti-Erk, and anti-actin antibodies.

[^{3}H]UTP/UTP exchange and to a lesser extent [^{3}H]TTP/TTP and [^{3}H]CTP/CTP exchange (Figure 6). Low or very low transport rates were observed for GTP, ATP, dATP, NAD, S-adenosylmethionine, citrate, and (not shown) several other nucleotides, amino acids, polyamines, and carboxylic acids. These data demonstrate that PNC1 is a pyrimidine nucleotide transporter of primarily UTP. This makes PNC1 different from its yeast counterpart Rim2p, which transports UTP, CTP, and TTP predominantly (Marobbio *et al.*, 2006).

PNC1 Suppression Decreases Accumulation of UTP in Mitochondria

We next investigated potential changes in cellular nucleotide levels as a mechanism for the effects of PNC1 on cell growth and proliferation. Suppression of PNC1 expression would be expected to reduce mitochondrial UTP, but it could also affect the cellular ATP:ADP ratio due to mitochondrial dysfunction. To test this, total cellular nucleotides were extracted from *pnc1* siRNA-transfected and control-transfected MCF-7 cells and quantified by HPLC analysis. The total amount of nucleotides extracted from *pnc1* siRNA transfected-MCF-7 cells was always lower than control cells due to a decrease in proliferation. Therefore, the GTP peak was used as an internal standard, and the quantity of other nucleotides was expressed as a percentage of GTP levels. The levels of total cellular UTP were not significantly altered in cells where PNC1 expression was repressed by siRNA, compared with the controls (Figure 7A). The ATP and ADP pools were also not significantly different and the ratio of ADP/ATP appeared to be unaltered.

Nucleotide levels were assessed in mitochondrial fractions isolated from cells by differential centrifugation. UTP

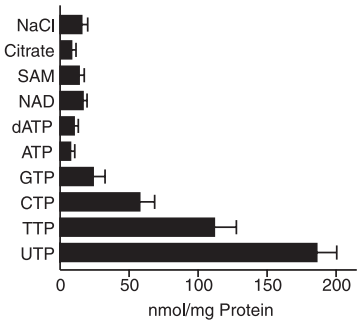

Figure 6. PNC1 is a pyrimidine nucleotide transporter with substrate selectivity for UTP. Transport was started by adding the indicated radioactive substrate (1 mM) to proteoliposomes reconstituted with recombinant PNC1 purified from *E. coli* (see *Materials and Methods*). Proteoliposomes contained the same substrate (unlabeled) at a concentration of 10 mM. With NaCl inside, the labeled substrate was 1 mM UTP. The data represent the means ± SEM of at least three independent experiments.

levels were significantly lower in *pnc1* siRNA-transfected MCF-7 cells compared with controls, whereas ADP, ATP, and GTP levels were not significantly altered (Figure 7B). The ADP:ATP ratio, which is higher in isolated mitochondria than in total cell extracts, was not altered by suppression of PNC1. Expression of the mitochondrial marker VDAC and the cytoplasmic marker paxillin in the same amount of total protein demonstrated that the mitochondrial fraction was uncontaminated (Figure 7C). Mitochondrial mass was not significantly altered in cells with suppressed PNC1 compared with controls (Figure 7D).

Overall, the data indicate that suppression of PNC1 expression causes decreased accumulation of UTP in mitochondria. This suggests that the effects of PNC1 suppression on cell growth are due to its function as a UTP carrier and that mitochondrial UTP levels may regulate cell growth.

PNC1 Expression Regulates Cellular ROS Levels

We next asked if suppressed PNC1 expression may elicit a mitochondrial retrograde or stress signaling response, which is associated with increased cellular ROS and has been proposed as an important mechanism of communication between mitochondria and nucleus in response to physiological and pathological stimuli (Biswas *et al.*, 1999; Amuthan *et al.*, 2002; Butow and Avadhani, 2004). To do this, cellular ROS levels were measured in cells with either increased or decreased PNC1 expression. As can be seen in Figure 8A, MCF-7 cells overexpressing PNC1 had decreased basal cellular levels of ROS compared with Vector controls in normal culture conditions. MCF-7 cells with suppressed PNC1 had increased cellular ROS compared with controls (Figure 8B). HeLa cells with stably suppressed PNC1 expression also had increased ROS levels (data not shown). These data indicate that cellular ROS levels are strongly influenced by PNC1 expression and suggest that

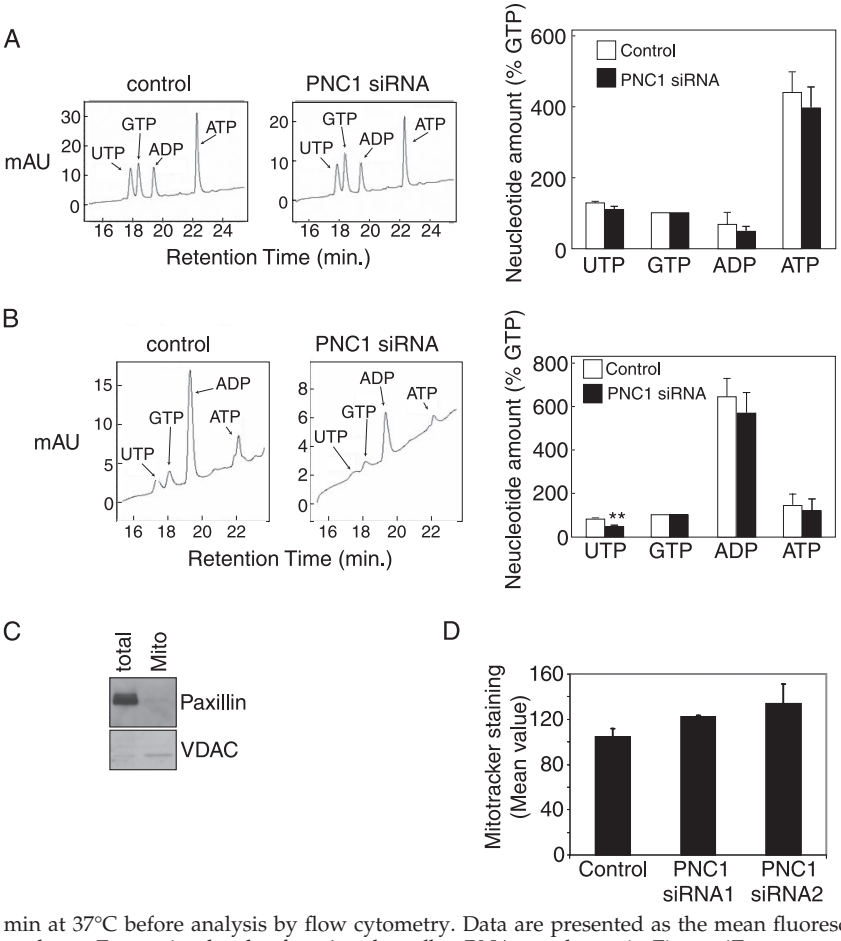

Figure 7. Suppression of PNC1 expression reduces UTP accumulation in mitochondria. (A) MCF-7 cells were transfected with siRNA directed toward *pnc1*or a control siRNA. After 48-h culture, cellular nucleotides were extracted as outlined in *Materials and Methods* and analyzed by reverse-phase HPLC using pure nucleotides as reference standards. The left and right panels are representative regions of the chromatograms for control siRNA and *pnc1* siRNA-transfected cells. The histogram represents the average amounts of nucleotides expressed as a percentage of GTP, which was set at 100% as an internal reference. Results represent the average of three transfected cell populations for the control and five separate transfected cell populations for the *pnc1*-specific siRNA, where *pnc1* mRNA levels were reduced by an average of 70% as measured by qPCR. Statistical significance of difference was evaluated using a Student's two-sided *t* test. (B) Mitochondria were extracted from MCF-7 cells transfected with either control or *pnc1* siRNA. Nucleotides were extracted and analyzed by HPLC as described above. Results are from three (negative control) or four (PNC1 siRNA) individually transfected cell populations where PNC1 levels were reduced by 70% as measured by qPCR. Statistical significance of difference was evaluated using a Student's two-sided *t* test, with $^{**}p < 0.001$. (C) Western blot analysis of cytoplasmic and mitochondrial fractions, showing the cytoplasmic marker paxillin and the mitochondrial marker VDAC. Gels were loaded with 30 μg total protein per fraction. (D) To measure mitochondrial mass, MCF-7 cells were transfected with siRNA directed toward *pnc1* or a control siRNA, and 72 h after transfection were incubated with MitoTracker dye (25 nM) for 30 min at 37°C before analysis by flow cytometry. Data are presented as the mean fluorescence obtained for each culture from three separate analyses. Expression levels of *pnc1* and *gapdh* mRNA are shown in Figure 4E.

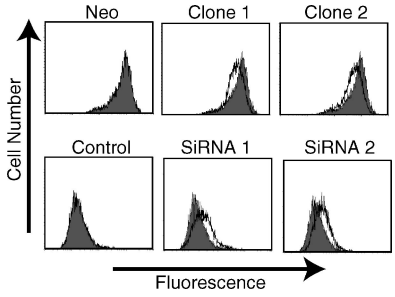

Figure 8. (Upper panels) MCF-7/Neo (control) and MCF-7/HaPNC1 cells were cultured in complete medium for 24 h, then washed, and incubated in PBS containing 10 μM H_2DCF-DA fluorescent probe for 15 min in the dark at 20°C. (Lower panels) MCF-7 cells were transfected with siRNA directed toward *pnc1* or a control siRNA. After 48-h culture, cells were washed and incubated in PBS containing 10 μM H_2DCFDA fluorescent probe for 15 min in the dark at 20°C. Cells were analyzed by flow cytometry, and the data are presented as a representative of three separate experiments with similar results. The solid histogram represents the control and the line represents the MCF-7/HaPNC1 cell clones in upper panels or the siRNA-transfected cells in lower panels.

PNC1 has a function in regulating mitochondrial retrograde signaling.

DISCUSSION

The contribution of mitochondria to the growth and proliferation of cancer cells and the integration of mitochondrial function with the IGF-I and mTOR signaling pathways, glycolysis, and energy metabolism is an important, but largely unexplored area of biology. Here, we have shown that insulin and IGF-I induce the expression of the mitochondrial pyrimidine nucleotide carrier PNC1. Suppression of PNC1 results in reduced mitochondrial UTP accumulation, reduced cell growth, and reduced cell proliferation. These findings suggest that enhanced expression of PNC1 is a mechanism by which mitochondrial activity contributes to the proliferation of transformed cells.

PNC1 expression is rapidly induced by both IGF-I and insulin, and this induction could be suppressed by inhibiting either PI-3 kinase or mTORC1 activity. The *pnc1* promoter contains several response elements that are known targets of the PI-3 kinase and mTOR pathway (Heinemeyer *et al.*, 1998). Several putative binding sites for transcription factors known to control the expression of genes encoding mitochondrial proteins (Sp1, NRF-2, and CREB; Scarpulla, 2002) were also observed in the promoter. Interestingly most of these are present in a small region near the transcription start site, which may indicate the presence of a proximal promoter. All of this suggests that PNC1 is a transcriptional target of the PI-3 kinase signaling pathway important for regulation of mitochondrial activity. Our data on enhanced expression of PNC1 in all transformed cell lines tested compared with nontransformed cells and in a panel of prostate carcinomas compared with normal prostate tissue suggest that PNC1 may be up-regulated to provide a growth advantage to cancer cells. This is in agreement with recent studies suggesting a central role for the mTORC1 signaling complex in oncongenesis. By using a series of murine models that are deficient in specific Akt isoforms, it was demonstrated that the requirement for Akt signaling to promote oncogenesis and cell proliferation is exclusively dependent on the activity of the mTORC1 (mTOR-Raptor) complex (Skeen *et al.*, 2006). Interestingly, we also observed increased PNC1 expression in tumor tissues of different origin and in prostate tissues exhibiting hyperplasia (data not shown). These observations suggest that increased expression of PNC1 may generally be associated with proliferating cells or may contribute to the early stages of malignant transformation.

Overexpression of PNC1 increased cell growth and suppression of PNC1 expression caused decreased cell growth. In MCF-7 cells this was accompanied by a decrease in the rate of progression through the cell cycle and overall decreased cell proliferation. The decreased cell growth may be a consequence of the retarded progression through the G1 phase of the cell cycle. However, although suppression of PNC1 caused decreased accumulation of UTP in the mitochondria, this was not accompanied by changes in the cellular ATP/ADP ratio or ATP levels. This suggests that the retarded cell cycle progression is not solely caused by altered cellular energy levels that could result from deceased ATP production by mitochondria and the consequent alterations in ADP and AMP levels.

The decreased size of cells with suppressed PNC1 expression prompted us to investigate the mTOR pathway as a target of the putative signal from mitochondria to the cell cycle. S6K1 and 4EBP1 have previously been shown to be dephosphorylated in response to disruption of mitochondrial function (Kim *et al.*, 2002) and the mTOR-raptor complex to be regulated in a redox-sensitive manner (Sarbassov and Sabatini, 2005). However, in agreement with our observations on unchanged ATP levels and mitochondrial mass, we did not observe any significant effect on phosphorylation of S6K1 or 4EBP1 in cells with suppressed PNC1. It has been proposed that a homeostatic regulatory loop exists between mTORC1 and mitochondria (Schieke and Finkel, 2006). In addition to mTORC1 activity being regulated by mitochondrial signals, the activation and stability of the mTORC1 complex has been correlated with increased oxidative phosphorylation and oxidative capacity (Schieke *et al.*, 2006). Overall, our data demonstrating induction of PNC1 in a mTORC1-dependent manner and the lack of effects of suppression of PNC1 on S6K1 and 4EBP1 phosphorylation support a role for mTORC1 as an upstream regulator of mitochondrial function.

Because there was no obvious effect on mitochondrial membrane potential or oxidative phosphorylation in cells with suppressed PNC1, we conclude that there was no gross mitochondrial dysfunction in these cells. However the effects of PNC1 suppression on cell cycle progression and cell size suggest that reduced PNC1 results in an inhibitory signal from mitochondria for cell growth and cell cycle progression. This signal may be a component of a mitochondrial retrograde signaling (mitochondrial stress signaling) response, which is thought to be an important mechanism of communication between mitochondria and nucleus in response to physiological and pathological stimuli (Biswas *et al.*, 1999; Amuthan *et al.*, 2002; Butow and Avadhani, 2004). Mitochondrial signaling has been associated with regulation of cell cycle progression (Boonstra and Post, 2004), with altered cytoplasmic calcium levels, production of ROS, altered stress kinase pathway activation, and altered nuclear gene transcription (Butow and Avadhani, 2004). Our data demonstrating decreased basal cellular ROS levels when PNC1 is overexpressed and increased ROS levels when PNC1 is suppressed suggest that PNC1 can regulate mitochondrial retrograde signaling. Increased cellular ROS levels have previously been shown to enhance or suppress cell cycle progression and signaling responses in cells (Boonstra and Post, 2004). In conditions where there is cell cycle arrest in G1, this may be associ-

ated with protection from oxidative damage and cell death (Rancourt *et al.*, 2002). The precise mechanism of the effects of PNC1-regulated ROS levels on cell growth remain to be determined as do the consequences of this for transformed cells. However, it is apparently not dependent on p53 function because similar effects were observed in HeLa cells, which do not express functional p53, and in MCF-7 cells.

Mitochondria may propagate retrograde signals as a mechanism of promoting adaptations to physiological changes that are sensed in cells. This possibility is receiving significant attention as a causative factor in ageing and lifespan regulation in simple organisms (Biswas *et al.*, 2005; Schieke and Finkel, 2006). Mitochondrial signals may also have a role in pathological adaptations such as in cancer progression. For example, in lung carcinoma cells mitochondrial retrograde signaling has been associated with induction of genes required for acquisition of an aggressive invasive phenotype (Biswas *et al.*, 2005).

PNC1 is the first mammalian mitochondrial carrier identified to have selectivity for pyrimidine nucleotides. It displays a distinct preference for UTP over TTP and CTP unlike the closely related yeast carrier Rim2p, which transports UTP, CTP, and TTP (Marobbio *et al.*, 2006). This suggests a more specialized function in mammalian cells than in yeast cells. However, it is likely that PNC1 is not solely responsible for transporting pyrimidine nucleotides into mitochondria, and there is compensatory activity by related isoforms or a carrier that can transport all purine and pyrimidine nucleotides without selectivity (Palmieri, 2004). This might also explain the lack of gross mitochondrial dysfunction in cells when PNC1 was suppressed.

In summary, we have demonstrated that PNC1 is a target of the IGF-I and insulin signaling pathway that functions in integration of growth factor signaling and mitochondria function with cell growth and proliferation. Increased expression of PNC1 in transformed cells suggests that PNC1 is important for the activity of mitochondria in the proliferation of cancer cells.

ACKNOWLEDGMENTS

We are grateful to Nancy Kedersha for assistance with immunofluorescence, Kurt Tidmore for preparing the illustrations, and to our colleagues for helpful discussions. This work was funded by Science Foundation Ireland, Enterprise Ireland, Irish Research Council for Science Engineering and Technology, Ministero dell' Università e della Ricerca, Apulia Region "Project Biotechnoter," Centro di Eccellenza di Genomica in campo Biomedico ed Agrario, and the European Community contract LSHM-CT-2004-503116. Edmund Kunji acknowledges the financial support of the Medical Research Council.

REFERENCES

Altomare, D. A., and Testa, J. R. (2005). Perturbations of the AKT signaling pathway in human cancer. Oncogene *24*, 7455–7464.

Amuthan, G., Biswas, G., Ananadatheerthavarada, H. K., Vijayasarathy, C., Shephard, H. M., and Avadhani, N. G. (2002). Mitochondrial stress-induced calcium signaling, phenotypic changes and invasive behavior in human lung carcinoma A549 cells. Oncogene *21*, 7839–7849.

Biswas, G., Adebanjo, O. A., Freedman, B. D., Anandatheerthavarada, H. K., Vijayasarathy, C., Zaidi, M., Kotlikoff, M., and Avadhani, N. G. (1999). Retrograde Ca2+ signaling in C2C12 skeletal myocytes in response to mitochondrial genetic and metabolic stress: a novel mode of inter-organelle crosstalk. EMBO J. *18*, 522–533.

Biswas, G., Guha, M., and Avadhani, N. G. (2005). Mitochondria-to-nucleus stress signaling in mammalian cells: nature of nuclear gene targets, transcription regulation, and induced resistance to apoptosis. Gene *354*, 132–139.

Boonstra, J., and Post, J. A. (2004). Molecular events associated with reactive oxygen species and cell cycle progression in mammalian cells. Gene *337*, 1–13.

Brand, K. A., and Hermfisse, U. (1997). Aerobic glycolysis by proliferating cells: a protective strategy against reactive oxygen species. FASEB J. *11*, 388–395.

Butow, R. A., and Avadhani, N. G. (2004). Mitochondrial signaling: the retrograde response. Mol. Cell *14*, 1–15.

Cully, M., You, H., Levine, A. J., and Mak, T. W. (2006). Beyond PTEN mutations: the PI3K pathway as an integrator of multiple inputs during tumorigenesis. Nat. Rev. Cancer *6*, 184–192.

Dougherty, D. A. (1996). Cation-pi interactions in chemistry and biology: a new view of benzene, Phe, Tyr, and Trp. Science *271*, 163–168.

Edinger, A. L., and Thompson, C. B. (2002). Akt maintains cell size and survival by increasing mTOR-dependent nutrient uptake. Mol. Biol. Cell *13*, 2276–2288.

Elbashir, S. M., Harborth, J., Lendeckel, W., Yalcin, A., Weber, K., and Tuschl, T. (2001). Duplexes of 21-nucleotide RNAs mediate RNA interference in cultured mammalian cells. Nature *411*, 494–498.

Fiermonte, G., Palmieri, L., Dolce, V., Lasorsa, F. M., Palmieri, F., Runswick, M. J., and Walker, J. E. (1998). The sequence, bacterial expression, and functional reconstitution of the rat mitochondrial dicarboxylate transporter cloned via distant homologs in yeast and *Caenorhabditis elegans*. J. Biol. Chem. *273*, 24754–24759.

Fiermonte, G., Walker, J. E., and Palmieri, F. (1993). Abundant bacterial expression and reconstitution of an intrinsic membrane-transport protein from bovine mitochondria. Biochem. J. *294*(Pt 1), 293–299.

Heinemeyer, T. *et al.* (1998). Databases on transcriptional regulation: TRANSFAC, TRRD and COMPEL. Nucleic Acids Res. *26*, 362–367.

Hofmann, F., and Garcia-Echeverria, C. (2005). Blocking the insulin-like growth factor-I receptor as a strategy for targeting cancer. Drug Discov. Today *10*, 1041–1047.

Kaplan, R. S. (2001). Structure and function of mitochondrial anion transport proteins. J. Membr. Biol. *179*, 165–183.

Kim, D. H., Sarbassov, D. D., Ali, S. M., King, J. E., Latek, R. R., Erdjument-Bromage, H., Tempst, P., and Sabatini, D. M. (2002). mTOR interacts with raptor to form a nutrient-sensitive complex that signals to the cell growth machinery. Cell *110*, 163–175.

Kunji, E. R. (2004). The role and structure of mitochondrial carriers. FEBS Lett. *564*, 239–244.

LeRoith, D., and Roberts, C. T., Jr. (2003). The insulin-like growth factor system and cancer. Cancer Lett. *195*, 127–137.

Lopez, T., and Hanahan, D. (2002). Elevated levels of IGF-1 receptor convey invasive and metastatic capability in a mouse model of pancreatic islet tumorigenesis. Cancer Cell *1*, 339–353.

Loughran, G., Healy, N. C., Kiely, P. A., Huigsloot, M., Kedersha, N. L., and O'Connor, R. (2005a). Mystique is a new insulin-like growth factor-I-regulated PDZ-LIM domain protein that promotes cell attachment and migration and suppresses anchorage-independent growth. Mol. Biol. Cell *16*, 1811–1822.

Loughran, G., Huigsloot, M., Kiely, P. A., Smith, L. M., Floyd, S., Ayllon, V., and O'Connor, R. (2005b). Gene expression profiles in cells transformed by overexpression of the IGF-I receptor. Oncogene *24*, 6185–6193.

Majewski, N., Nogueira, V., Bhaskar, P., Coy, P. E., Skeen, J. E., Gottlob, K., Chandel, N. S., Thompson, C. B., Robey, R. B., and Hay, N. (2004). Hexokinase-mitochondria interaction mediated by Akt is required to inhibit apoptosis in the presence or absence of Bax and Bak. Mol. Cell *16*, 819–830.

Marobbio, C. M., Di Noia, M. A., and Palmieri, F. (2006). Identification of a mitochondrial transporter for pyrimidine nucleotides in *Saccharomyces cerevisiae*: bacterial expression, reconstitution and functional characterization. Biochem. J. *393*, 441–446.

Palmieri, F. (1994). Mitochondrial carrier proteins. FEBS Lett. *346*, 48–54.

Palmieri, F. (2004). The mitochondrial transporter family (SLC25): physiological and pathological implications. Pfluegers Arch. *447*, 689–709.

Palmieri, F., Indiveri, C., Bisaccia, F., and Iacobazzi, V. (1995). Mitochondrial metabolite carrier proteins: purification, reconstitution, and transport studies. Methods Enzymol. *260*, 349–369.

Palmieri, L., Runswick, M. J., Fiermonte, G., Walker, J. E., and Palmieri, F. (2000). Yeast mitochondrial carriers: bacterial expression, biochemical identification and metabolic significance. J. Bioenerg. Biomembr. *32*, 67–77.

Pebay-Peyroula, E., Dahout-Gonzalez, C., Kahn, R., Trezeguet, V., Lauquin, G. J., and Brandolin, G. (2003). Structure of mitochondrial ADP/ATP carrier in complex with carboxyatractyloside. Nature *426*, 39–44.

Plas, D. R., Talapatra, S., Edinger, A. L., Rathmell, J. C., and Thompson, C. B. (2001). Akt and Bcl-xL promote growth factor-independent survival through distinct effects on mitochondrial physiology. J. Biol. Chem. *276*, 12041–12048.

Plas, D. R., and Thompson, C. B. (2005). Akt-dependent transformation: there is more to growth than just surviving. Oncogene *24*, 7435–7442.

Rancourt, R. C., Hayes, D. D., Chess, P. R., Keng, P. C., and O'Reilly, M. A. (2002). Growth arrest in G1 protects against oxygen-induced DNA damage and cell death. J. Cell. Physiol. *193*, 26–36.

Samuels, Y., and Ericson, K. (2006). Oncogenic PI3K and its role in cancer. Curr. Opin. Oncol. *18*, 77–82.

Sarbassov, D. D., and Sabatini, D. M. (2005). Redox regulation of the nutrient-sensitive raptor-mTOR pathway and complex. J. Biol. Chem. *280*, 39505–39509.

Scarpulla, R. C. (2002). Transcriptional activators and coactivators in the nuclear control of mitochondrial function in mammalian cells. Gene *286*, 81–89.

Schieke, S. M., and Finkel, T. (2006). Mitochondrial signaling, TOR, and life span. Biol. Chem. *387*, 1357–1361.

Schieke, S. M., Phillips, D., McCoy, J. P., Jr., Aponte, A. M., Shen, R. F., Balaban, R. S., and Finkel, T. (2006). The mammalian target of rapamycin (mTOR) pathway regulates mitochondrial oxygen consumption and oxidative capacity. J. Biol. Chem. *281*, 27643–27652.

Schmelzle, T., and Hall, M. N. (2000). TOR, a central controller of cell growth. Cell *103*, 253–262.

Sell, C., Dumenil, G., Deveaud, C., Miura, M., Coppola, D., DeAngelis, T., Rubin, R., Efstratiadis, A., and Baserga, R. (1994). Effect of a null mutation of the insulin-like growth factor I receptor gene on growth and transformation of mouse embryo fibroblasts. Mol. Cell. Biol. *14*, 3604–3612.

Skeen, J. E., Bhaskar, P. T., Chen, C. C., Chen, W. S., Peng, X. D., Nogueira, V., Hahn-Windgassen, A., Kiyokawa, H., and Hay, N. (2006). Akt deficiency impairs normal cell proliferation and suppresses oncogenesis in a p53-independent and mTORC1-dependent manner. Cancer Cell *10*, 269–280.

Titus, S. A., and Moran, R. G. (2000). Retrovirally mediated complementation of the glyB phenotype. Cloning of a human gene encoding the carrier for entry of folates into mitochondria. J. Biol. Chem. *275*, 36811–36817.

Todisco, S., Agrimi, G., Castegna, A., and Palmieri, F. (2006). Identification of the mitochondrial NAD+ transporter in *Saccharomyces cerevisiae*. J. Biol. Chem. *281*, 1524–1531.

Van Dyck, E., Jank, B., Ragnini, A., Schweyen, R. J., Duyckaerts, C., Sluse, F., and Foury, F. (1995). Overexpression of a novel member of the mitochondrial carrier family rescues defects in both DNA and RNA metabolism in yeast mitochondria. Mol. Gen. Genet *246*, 426–436.

Wang, B., Li, N., Sui, L., Wu, Y., Wang, X., Wang, Q., Xia, D., Wan, T., and Cao, X. (2004). HuBMSC-MCP, a novel member of mitochondrial carrier superfamily, enhances dendritic cell endocytosis. Biochem. Biophys. Res. Commun. *314*, 292–300.

Warburg, O. (1924). Uber den Stoffwechsel der Carcinomzelle. Biochem. Z. *152*, 309–344.

Warburg, O., Posener, K., and Negelein, E. (1930). The Metabolism of Tumours, London: Arnold Constable.